Spin and Molecular Dynamics of Biradicals as Studied by Low Field Nuclear Polarization at Variable Temperature

Alexandra Yurkovskaya,* Stefan Grosse, Sergey Dvinskikh, Olga Morozova,† and Hans-Martin Vieth*

Institute of Experimental Physics, Free University of Berlin, Arnimallee 14, D-14195 Berlin, Germany

Received: September 8, 1998

^{1}H and ^{13}C chemically induced dynamic nuclear polarization (CIDNP) and time-resolved stimulated nuclear polarization (SNP) have been applied to the investigation of spin and molecular dynamics in biradicals, generated in the photolysis of 2,2,12,12-tetramethylcyclododecanone, at low magnetic field in the temperature range from 200 to 360 K. This reaction involves two consecutive biradical stages, the primary acyl−alkyl and the secondary bis-alkyl biradical, with different reaction products. Characteristic differences in the CIDNP field dependencies and SNP decay times for nuclei of different reaction products are seen at high temperatures. Upon cooling, the emission maximum position shifts to low field and the width of the ^{1}H CIDNP field dependencies of the acyl−alkyl biradical products decreases. Below 243 K these effects reverse direction, furthermore, a significant slowing down of the SNP decay is observed. Calculations of the ^{1}H and ^{13}C CIDNP field dependencies and the SNP kinetics for the primary biradical have been performed based on the numerical solution of the stochastic Liouville equation for the biradical spin density matrix. They use a model of restricted diffusion for the description of the molecular dynamics and take into account the distance dependence of the exchange interaction. Good quantitative agreement between the calculations and experimental data is found for the whole temperature range when using the appropriate dependence of some of the parameters on temperature. In particular, it was necessary for the quantitative simulation in the low temperature range to introduce a temperature dependence of the biradical reactivity. The model calculations qualitatively confirm that the low-temperature broadening of the CIDNP field dependencies, and the increase of the SNP decay time are caused by the slowing down of the molecular mobility and the decreasing of reactivity. For the products of the secondary biradical, a qualitative interpretation is given showing that in comparison with the products of the primary biradical spin−orbit interaction is of less importance for the biradical spin dynamics, that the influence of the molecular mobility under the temperature variation is more pronounced, that the lifetime is longer, and that the nuclear polarization is more efficiently formed.

Introduction

Radical pairs (RPs) are important intermediates in many chemical reactions in solution. Being initially formed in a state of certain multiplicity (singlet or triplet), they can react usually only from their singlet state. Singlet−triplet transition in the radical pairs, which is dependent on such magnetic interactions as electron−nuclear hyperfine interaction (hfi), electron Zeeman interaction, and exchange interaction, can act as a bottleneck for chemical reactions and give rise to spin and magnetic field effects in chemical reactions in solution.[1] Flexible biradicals (**B**) generated during the photolysis of cyclic ketones (**K**) serve as a model system for many investigations of magnetic field and spin effects in radical reactions in our and several others laboratories.[2−7] In the present study, we extend our investigation to the case of photoreactions with two consecutive biradicals, $\mathbf{B_1}$ and $\mathbf{B_2}$, as intermediates, where the latter is formed from the former via the decarbonylation reaction, as shown is Scheme 1, where $\mathbf{P_1}$ and $\mathbf{P_2}$ is the set of products from the primary and the secondary biradicals, respectively.

In such a system, the magnetic field and spin effects reflect the complex interplay of spin, molecular and chemical dynamics of biradicals.[8] These effects are very sensitive to the molecular and spin dynamics of the RP partners; therefore, the study of their dependence on the magnetic resonance parameters and on the properties of the reaction media opens the opportunity to study the mechanisms of the elementary steps of chemical reactions.

The radical centers of the biradicals are linked by a polymethylene chain; as a result, no diffusive separation of the centers can occur, hence the average exchange integral $\langle J \rangle$ in such biradicals is much higher than that in ordinary radical pairs. The condition for spin polarization effects at low magnetic field comparable with $\langle J \rangle$ is particularly favorable due to crossing of the T_ and S levels, providing an efficient channel of singlet−triplet conversion. In this conversion, the total electron−nuclear spin is conserved and therefore it is accompanied by a nuclear spin flip. As a consequence, strong nuclear spin polarization of the products is observed in this magnetic field range. The chain dynamics, which varies the distance between the radical centers, modulates the exchange interaction $J(r)$, and consequently, affects the rate of triplet−singlet conversion and thus the spin dynamics of the biradicals. In this paper we concentrate our efforts on studies of nuclear spin polarization (CIDNP) at low magnetic field under variation of the temperature over a wide range. Time-resolved stimulated nuclear polarization (SNP) is

† International Tomography Center, Institutskaya 3a, 630090 Novosibirsk-90, Russia.

10.1021/jp9836325 CCC: $18.00
Published on Web 02/03/1999

also used with pulsed irradiation of a strong radio frequency (rf) field near the spin-resonance of paramagnetic intermediates.[9] Because of the complexity of the process of polarization formation, a sufficiently large database is needed for the unambiguous discrimination between the effects of molecular and of spin dynamics. The approach in our present study is to measure both, CIDNP field dependencies under cw light irradiation and transient SNP effects, and to vary the temperature and the viscosity of the solvents over a wide range. Since the chemical transformation of the primary biradical to the secondary one is strongly dependent on temperature, one can shorten the lifetime of the primary biradicals (**B_1**) by raising the temperature. By increasing the viscosity of the solvent or by lowering the temperature, we slowed the molecular chain mobility.

Furthermore, ^{1}H results are compared with ^{13}C results measured on compounds with natural isotope composition and on compounds deuterated in their methyl groups. Such a comparison allows us to vary the effective hyperfine interaction by studying proton and ^{13}C spin polarization effects for different atomic positions of the reaction products and by the isotope substitution. In combination with variation of the experimental conditions, we get the possibility to elucidate the effect of the chemical, spin and molecular dynamics on the evolution of intermediate biradicals.

For the theoretical description of the reaction process the numerical solution of the stochastic Liouville equation for the density matrix has been found to be successful for giving a realistic picture, in particular when the flexibility of the biradical is adequately modeled taking into account the distance dependence of the exchange interaction and its modulation by the molecular motion of the polymethylene chain.[5,10] Following this approach a major objective of our study is to obtain a simulation of all obtained experimental data by one common set of parameters and, in this way, to check the consistency of the model and its validity in the full range of temperature and viscosity.

Experimental Section

The ^{1}H and ^{13}C CIDNP and SNP experiments were performed on a custom built FT NMR spectrometer (7 T) allowing magnetic field cycling by using a pneumatic probe transfer system with a transfer time of 1−2 s.[11a,11b] The photochemical reaction was carried out in the low magnetic field of a current controlled electromagnet in the range of 0−0.13 T in a double-tuned NMR probe (300 MHz for ^{1}H and 75.4 for ^{13}C NMR detection). The sample was irradiated for 1−2 s at a pulse repetition frequency of 10−20 Hz by a Lambda Physik excimer laser ($\lambda = 308$ nm, pulse duration 15 ns (fwhm), and energy per pulse 5 mJ at the sample position). After irradiation at low field, the sample was transferred to the spectrometer magnet where the ^{1}H or ^{13}C NMR spectra of the polarized products were detected. The temperature variable studies were performed using a sample chamber with Styrofoam insulation and N_2 gas flow. The temperature was monitored by a calibrated platinum resistance thermometer located near the sample ampule. The instability and the gradient of the temperature across the sample volume did not exceed 1 K. For our setup with cycling the magnetic field by shuttling the whole probe high viscosity does not pose any limitation for low-field measurements, in contrast to experiments employing a flow system.

In the time-resolved SNP experiments we varied the delay between the laser pulse and the radio frequency pumping pulse. A long pulse (of about 2 μs) the duration of which was longer than the SNP decay or a short pulse (fwhm of about 20 ns) was used. The timing and shape of the rf-pulse were controlled with a pickup antenna positioned near the rf coil and monitored by a digital oscilloscope. The frequency for pumping the electron spin transitions was $\nu_{rf} = 300$ MHz. The amplitude B_1 of the rf magnetic field was calibrated by measuring the length of a $\pi/2$ NMR pulse for protons at 300 MHz. The time resolution of about 15 ns was mainly limited by the width of the rf pulse edges and by the length of the laser pulse. Numerical deconvolution of the SNP signal with the rf pulse shape allowed an improvement of the time resolution up to 5 ns. The amplitude of the SNP signal is given by the intensity difference of corresponding lines in the NMR spectra with and without rf irradiation.

SCHEME 1

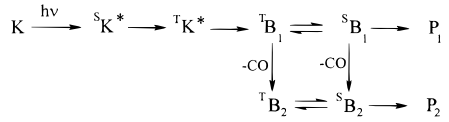

SCHEME 2

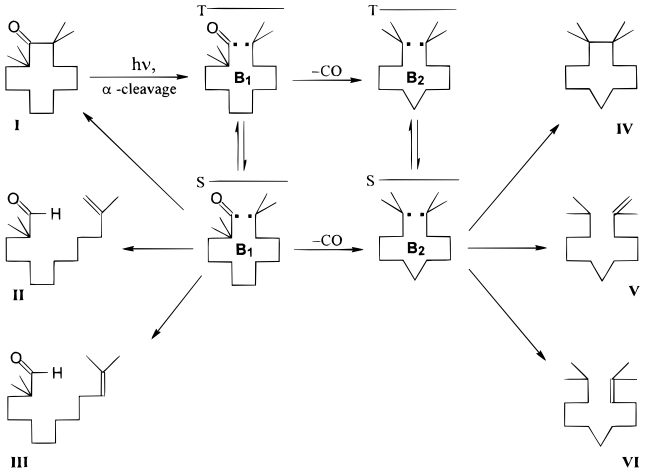

The cyclic aliphatic ketones 2,2,12,12-tetramethylcyclododecanone (**I**) and the analogous compound deuterated in its four α-methyl group positions (**I**-D_{12}), were kindly provided by Herbert Zimmermann (Max Planck Institute, Heidelberg, Germany). Deuterated solvents (methanol, ethanol, chloroform, toluene, and benzene) were obtained from Aldrich. Prior to irradiation, the solutions of 0.05M were bubbled with argon or helium for 5 min.

Results

Room temperature ^{1}H and ^{13}C CIDNP experiments at high and low magnetic fields were described and discussed in our recent publication,[8a] where the scheme of the photolysis of the starting ketone **I** (Scheme 2) was established. Products **I**−**III** are formed from the primary acyl−alkyl biradical **B_1**, which can also undergo the decarbonylation reaction resulting in the formation of the secondary bis-alkyl biradical **B_2**. Recombination and disproportionation of the biradical **B_2** leads to the formation of products **IV**, **V**, and **VI**. At ambient temperature the rate constant for the decarbonylation reaction estimated from high field CIDNP kinetics is $k_{co} = 3 \times 10^5$ s^{-1}.[8a] It is much smaller than the rate constant $k_1 = 1.5 \times 10^7$s^{-1} for the acyl−alkyl biradical lifetime as estimated from ESR measurements.[3a] Accordingly, the quantum yield for forming the secondary product is small.[4] Increase of the temperature accelerates the

decarbonylation reaction, and hence, the quantum yield of products **IV**−**VI** becomes higher. Thus, it is appropriate to combine all the results obtained in three groups with respect to temperature, data taken at room temperature, in a low (203−295 K) and in a high (295−365 K) temperature range.

^{1}H CIDNP. All eight β-protons (2 CH_3− and −CH_2−) of the alkyl end of acyl−alkyl and bis-alkyl biradicals exhibit scalar hyperfine coupling constants of approximately 2.2 mT.[12] At low magnetic field the CIDNP effect is emissive, corresponding to the efficient T_α−Sβ transitions of spin-selective intersystem conversion, where α and β denote the nuclear spin projection. ^{1}H CIDNP spectra exhibit three intense emissive lines: a signal of the aldehyde proton (−COH) of the products **II** and **III**, a signal of vinyl protons (=CH_2) of the products **II** and **V**, and an unresolved signal in the aliphatic region for the protons (−CH_3 and −CH_2−) of the starting ketone, as well as of the other reaction products. The polarization of the aldehyde proton is formed in the acyl−alkyl biradical only, while both $\mathbf{B}_1$ and $\mathbf{B}_2$ biradicals contribute to the polarization signal of vinyl and aliphatic protons.

Figure 1 b shows the CIDNP field dependencies for aldehyde and vinyl protons at room temperature normalized with respect to the value at the emission maximum. For the aldehyde proton, where published data are available, the field dependence is consistent with the previous results.[8] For the characterization of the field dependencies we use two parameters, the position of emissive maximum, B_0^{max}, and the width (fwhm) ΔB. At temperatures above room temperature a considerable increase of the width ΔB and a shift of the B_0^{max} toward higher field is observed for =CH_2 and −CH_3 protons (not shown), while the changes in the CIDNP field dependence for the −COH proton are less pronounced. At 273 K and below, the field dependencies for the three groups of protons coincide within the experimental error. Upon cooling below room temperature, B_0^{max} is shifted toward low field. For the aldehyde proton signal, which was measured down to 200 K, B_0^{max} and ΔB reach their smallest value at a temperature of about 243 K with a sharp increase at further cooling (Figure 2).

^{13}C CIDNP. For the acyl−alkyl and the bis-alkyl biradical,

$$O{=}\underset{1}{\dot{C}}-\underset{2}{C}(CH_3)_2-((CH)_2)_9-\underset{12}{\dot{C}}(CH_3)_2$$

acyl−alkyl

$$\underset{1}{\dot{C}}(CH_3)_2-((CH)_2)_9-\underset{11}{\dot{C}}(CH_3)_2$$

bis-alkyl

the hyperfine interaction constants can be estimated from the values of the corresponding monoradicals: $A_{1-C} = 11.4$ mT, $A_{2-C} = 4.7$ mT, $A_{12-C} = 4.6$ mT, and $A_{1-C} = A_{11-C} = 4.6$ mT, respectively.[12] At natural abundance (1.1%) of the magnetic isotope ^{13}C, CIDNP effects are expected in each of these positions in the biradicals and in the corresponding position in the products, but not in two or more positions of one molecule simultaneously.

^{13}C CIDNP spectra obtained during the photolysis of **I** at room temperature at a field of 2.1T and 20 mT were discussed previously.[8a] In the present study we found that for **I**-D_{12} CIDNP effects are much stronger. In addition to five lines observed for **I**-H_{12} (signals 1−5 in Figure 3), three extra lines of small amplitude (signals 6−8) were detected for **I**-D_{12}. The line assignment is given in the top part of Figure 3.

All ^{13}C polarized signals exhibit emissive phase in the studied magnetic field range (0−120 mT) in accordance with the T_-S-mechanism of forming nuclear polarization. At room temperature, two types of field dependencies can be distinguished

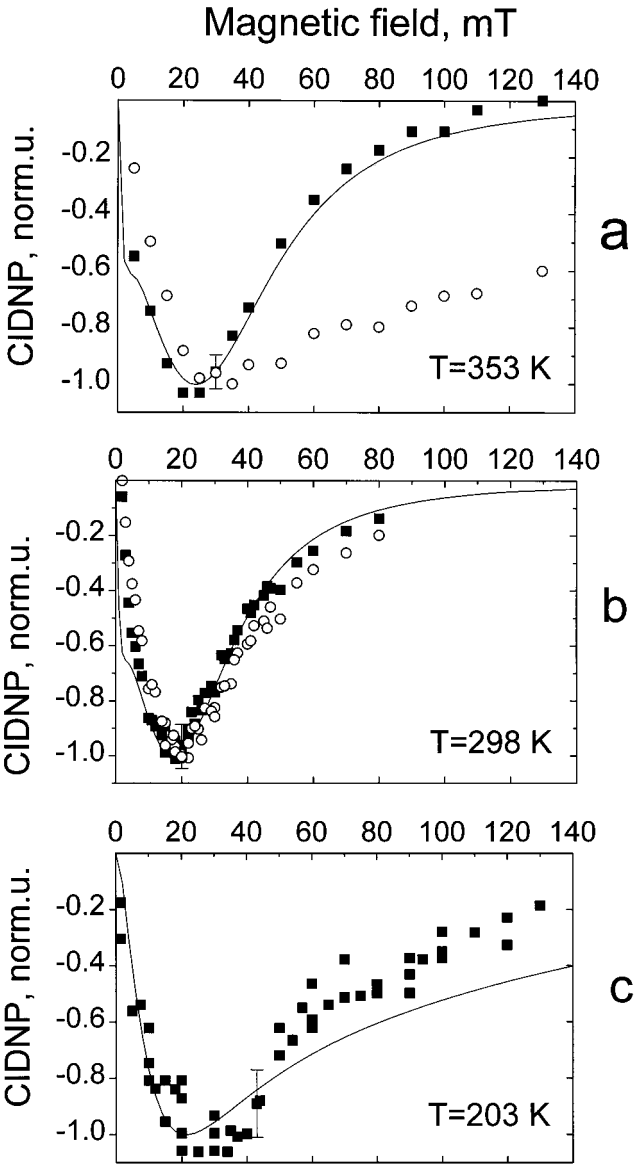

Figure 1. Normalized ^{1}H CIDNP field dependence of 0.05 M 2,2,-12,12-tetramethyl-cyclododecanone (a) in deuterated toluene at 353 K; (b) in deuterated methanol at room temperature, (c) in deuterated methanol at 203 K. (■) −COH proton, (○) =CH_2 protons, (−) model calculations with $A = 3.0$ mT; the other parameters are listed in Tables 1 and 2 for the corresponding temperatures.

(Figure 4). The first one with B_0^{max} around 20 mT is detected for signals 3−5, which correspond to the 2-C and 12-C atoms of the acyl−alkyl biradical. The second type of ^{13}C CIDNP field dependence is characterized by having B_0^{max} at 40 mT and a width ΔB of about 80 mT. It is observed for signals 1 and 2, which correspond to the carbonyl carbon atom in the acyl−alkyl biradical.

As in the case of ^{1}H CIDNP, decreasing the temperature below room-temperature shifts B_0^{max} of the ^{13}C polarization of signals 3−5 to lower magnetic field. Also, the width ΔB decreases monotonically with cooling, down to 243 K. At room temperature and below, the field dependencies for all these signals (3−5) coincide within the experimental error. Above room temperature, heating leads to the shift of B_0^{max} to higher field for signals 4 and 5. For signal 3, which has contribution from two products (**II** and **V**), such heating does not only shift B_0^{max} to higher magnetic field but also enhances the high field part of the CIDNP curve (see Figure 4).

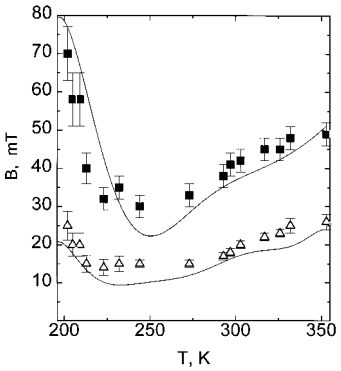

Figure 2. Temperature dependence of the emission maximum position B_0^{max} (△) and the width ΔB (■) of the ^{1}H CIDNP field dependence of −COH protons in deuterated methanol, (−) corresponding calculation for $A = 3.0$ mT. For details of calculations see the text.

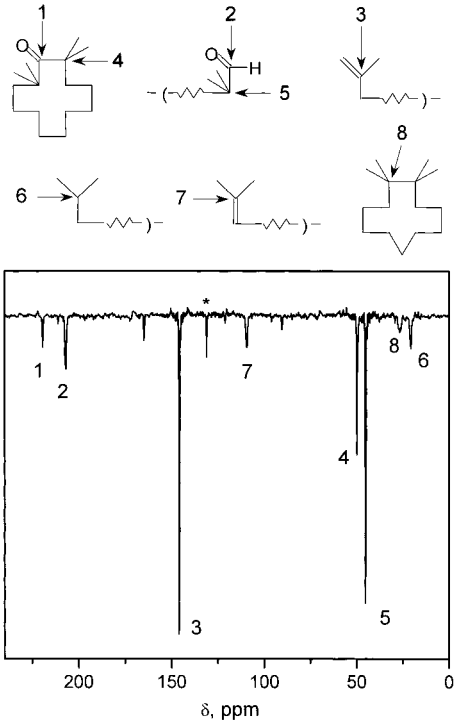

Figure 3. ^{13}C CIDNP spectrum at $B_0 = 20$ mT obtained during the photolysis of **I**-D_{12} at room temperature in ethanol ((∗) center of the spectrum).

Time-Resolved SNP. Radio frequency pumping induces spin transitions in the triplet manifold of the biradicals. The transitions replenish the preferentially depopulated T_α level, hence, rf pumping increases the number of biradicals undergoing the T_α-Sβ conversion and, as a consequence, enhances the emissive amplitude of CIDNP. The dependence of the SNP signals on the external magnetic field strength at constant rf frequency (SNP spectrum) exhibits a well pronounced emissive maximum with its position dependent on the hfi constant. To obtain quantitative information on the kinetics of the reaction, we measured the ^{1}H and ^{13}C SNP time decay at the field corresponding to the maximum in the SNP spectra.

For quantitative analysis we introduced a normalized measure of SNP,[11a]

$$K_{SNP} = \frac{I_S - I_C}{I_C - I_D}$$

where I_S and I_C are the line intensity with and without rf pumping, and I_D is the "dark" magnetization measured in the absence of light excitation. At our experimental conditions, K_{SNP} is independent of such experimental parameters as duration and intensity of light irradiation, optical density of the solution, sample transfer time, and nuclear relaxation time; it characterizes the SNP effect for a given setting of the rf excitation parameters.

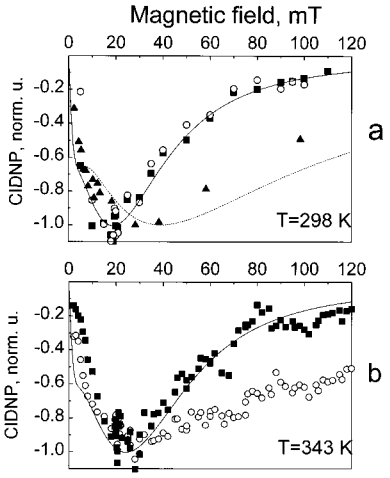

Figure 4. ^{13}C CIDNP field dependence for signals (○) 3, (■) 5, and (▲) 2, at (a) room temperature and at (b) 353 K. (−) Calculation with $A = 4.6$ mT (solid) and $A = 11.4$ mT (dashed), the other parameters are listed in Table 1 and Table 2 for 289 K and for 353 K.

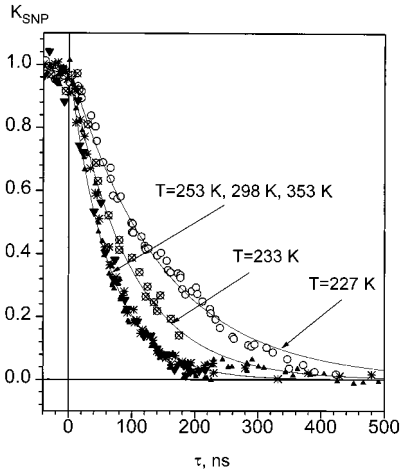

Figure 5. ^{1}H SNP decay of aldehyde proton at different temperatures ((○) 227 K, (⊗) 233 K, (▼) 253 K, (∗) 298 K, (▲) 353 K). Solid lines are exponential functions with decay times 67, 90, and 144 ns.

In the ^{1}H SNP spectrum the maximum was observed at 10.7 mT. At room temperature, there were no significant differences in the initial SNP amplitude ($K_{SNP}(t=0) = K^0_{SNP}$) and SNP signal decay time for different lines in the CIDNP spectrum. As the temperature increases the SNP signal decay of the $=CH_2$ and $-CH_3$ signals becomes slower, while the decay time of the aldehyde proton does not change upon heating (Figure 6b). The decay time for the aldehyde proton at 353 K is 59 ± 5 ns with the initial amplitude $K^0_{SNP} = 0.32$. The best fit for $=CH_2$ protons is obtained assuming a sum of two exponential decays, one having the same amplitude and decay time as the aldehyde signal ($K^0_{SNP} = 0.32$) and the another one with a decay time of 166 ± 5 ns and $K^0_{SNP} = 0.49$. At low temperatures (below 250 K), only the slowly relaxing −COH signal can be measured with sufficient accuracy. When cooling below 233 K, the SNP decay of the aldehyde proton becomes significantly slower. Figure 5 shows the SNP decay (with normalized amplitude) of the aldehyde peak. It can be described by a

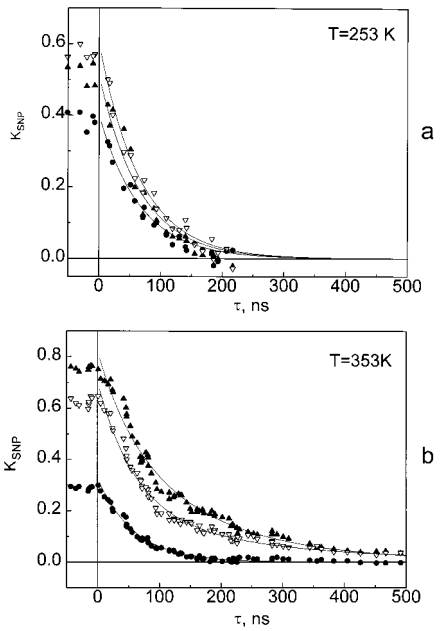

Figure 6. ^{1}H SNP for (△) $-CH_3$ protons, (●) aldehyde protons, and (▲) $=CH_2$ protons: (a) at 253 K and (b) at 353 K. Solid line for (a) is an exponential function with a decay time of 67 ns. Solid lines on (b) are the fit functions described in the text, $B_0 = 10.7$ mT, $B_1 = 0.6$ mT. τ is the delay between the laser flash and the beginning of the radio frequency pulse.

monoexponential decay with the time constant 65, 82, and 144 ns at 298, 233, and 227 K, respectively. Also the initial SNP amplitude K^0_{SNP} is slightly reduced from 0.4 at room temperature to 0.25 at 233K.

Time-resolved ^{13}C SNP measurements were performed for the strongest signals (3−5) in the CIDNP spectra and only at room temperature. The ^{13}C SNP decays for the signals 3−5 coincide with each other (not shown) and nearly coincide with the decay of the SNP signal for protons.

Model Calculations. Our calculations of CIDNP and SNP were based on the approach of de Kanter[5] for the description of the CIDNP field dependencies in the geminate recombination of biradicals, which involves the numerical solution of the stochastic Liouville equation (SLE):

$$\frac{\partial\rho(t)}{\partial t} = -i\hat{\mathbf{L}}\rho(t) + \hat{\mathbf{R}}\rho(t) + \hat{\mathbf{W}}\rho(t) + \hat{\mathbf{K}}\rho(t) \qquad (1)$$

Here $\hat{\mathbf{L}}$ is the Liouville operator which is associated with the spin Hamiltonian H in accordance with the equation $\hat{L}\rho(t) = \hat{H}\rho(t) - \rho(t)\hat{H}$, $\hat{\mathbf{R}}$ is the relaxation matrix, $\hat{\mathbf{W}}$ characterizes the dynamic behavior of the polymethylene chain, and $\hat{\mathbf{K}}$ represents the chemical reactions of the biradicals. In the scope of this article we restrict ourselves to a few remarks and the general concepts of this approach, and we refer the readers to previous publications, where a detailed description is given.[5,8b]

The spin Hamiltonian includes the Zeeman interaction with the external magnetic field B_0 of the paramagnetic centers having g factors g_1 and g_2, the electron−nuclear hyperfine interaction with the hyperfine coupling constant A, and the exchange interaction between the unpaired electrons $J(r)$:

$$\hat{H} = \beta_e\hbar^{-1}B_0(g_1\hat{S}_{1z} + g_2\hat{S}_{2z}) + A\hat{S}_{1z}\hat{I}_z + A(\hat{S}_{1x}\hat{I}_x + \hat{S}_{1y}\hat{I}_y) - J(r)(^1/_2 + 2\hat{S}_1\cdot\hat{S}_2) \qquad (2)$$

With present computers for the reason of practicability, this approach does not allow the calculation of low-field effects with taking into account all magnetic nuclei within a reasonable time, because the dimensions of the resulting matrixes become too large. In our present calculations the magnetic interactions of the electron with all nuclei are therefore replaced by the interaction with only one nuclear spin $^1/_2$ having the effective hfi constant $A_{eff} = A$. The direct products of the electronic and the nuclear spin functions are used as a basis of the Liouville space (Sα, T$_0\alpha$, T$_+\alpha$, T_α, Sβ, T$_0\beta$, T$_+\beta$, T_β) and all electron−nuclear transitions are taken into account.

The exchange interaction is assumed to depend exponentially on the biradical end-to-end distance r:

$$J(r) = J_0e^{-\alpha r} \qquad (3)$$

For the description of the conformational motion of the polymethylene chain of the biradical, an end-to-end distance distribution function $C(r)$ was calculated.[5] We used a calculation based on the Monte Carlo computer program for simulation of *n*-alkanes developed by Lal and Spenser.[14] The conformation energy U_k is composed of the bond rotational energies and the energy due to the interaction among nonbonded atoms in the molecule. Parameters of the potential functions were taken according to Lal and Spenser.[14.] From the energies U_k and the end-to-end distances r_k for 10^5 conformations, the distribution function r was calculated. The normalized distribution function $C(r)$ is divided into $m = 200$ segments of equal area. Transitions between neighboring segments i and k are described by the $\hat{\mathbf{W}}$ matrix:

$$W_{ik} = W_{ki} = \frac{D'}{(r_i - r_k)^2} \qquad (4)$$

where D' is the effective diffusion coefficient and r_i is the average end-to-end distance for segment i.

For the description of the relaxation, the motion of the radical centers on the chain is divided into two contributions: the reorientation of the biradical as a whole and the local motion of the individual radical centers.[5] Consequently, the $\hat{\mathbf{R}}$ matrix consists of elements representing two different mechanisms of spin relaxation:[5] (i) interactions with no correlation between the two radical sites. They will be represented by fluctuating local magnetic fields $B_i(i = x, y, z)$ with correlation time τ_u. The usual relaxation processes operative in free radicals (electron−nuclear dipole interaction, hfi and g tensor anisotropy, etc.) are lumped together in fluctuating magnetic fields $B_i(i = x, y, z)$ which are uncorrelated at the two radical sites and are therefore independent of the chain conformation. The spectral density of the correlation function is described by $L(\omega)=2G\tau_u/(1 + \omega^2\tau_u^2)$, with $G = {}^1/_2g^2\beta_e|B_i|^2$. In the calculation of matrix elements for this mechanism within the frame of the Redfield relaxation theory, we followed ref 5 taking into account additional elements[10] erroneously missing in ref 5, and (ii) correlated dipole−dipole interaction between the two electron spins, characterized by the correlation time τ_c of the reorientation of the whole biradical in the solvent. This contribution is distant dependent; therefore, the corresponding matrix elements of $\hat{\mathbf{R}}$ are calculated for the average end-to-end distance r_i for each segment i of $C(r)$.

The $\hat{\mathbf{K}}$ matrix takes the following chemical reactions of the biradicals into account: (a) recombination of biradicals from the singlet state at the smallest end-to-end distance $r = r_d$, with rate constant k_r; (b) "scavenging" reactions, removing biradicals from geminate recombination, disregarding their spin state and end-to-end distance, with the rate constant k_{sc} (it includes decarbonylation, reactions with radical scavengers

or solvent impurities, etc.); and (c) biradical decay due to spin−orbit coupling. It is taken into account as biradical recombination from triplet substates T_i (T_0, T_+, T_-) at $r = r_d$, with rate constant k_{soc}.

We assume that the photolysis of the starting ketones produces biradicals having equally populated triplet sublevels and $r = r_d$ at $t = 0$.

For the calculation of the stationary CIDNP amplitude and its dependence on the magnetic field, the stochastic Liouville equation is solved by using the Laplace transformation of the spin density matrix, $\rho(s) = \int_0^\infty \rho(t)e^{-st}dt$, which yields the equation for the spin density matrix in the s domain:[5]

$$s\rho(s) + i\hat{\mathbf{L}}\rho(s) - \hat{\mathbf{R}}\rho(s) - \hat{\mathbf{W}}\rho(s) - \hat{\mathbf{K}}\rho(s) = \rho^0 \quad (5)$$

where $\rho^0 = \rho(t = 0)$.

The stationary CIDNP amplitude I was calculated according to eq 6:

$$I(s) = k_r[\rho_{S\alpha S\alpha}(s)|_{r=r_d} - \rho_{S\beta S\beta}(s)|_{r=r_d}] + k_{soc}\sum_i [\rho_{T_i\alpha T_i\alpha}(s)|_{r=r_d} - \rho_{T_i\beta T_i\beta}(s)|_{r=r_d}] \quad (6)$$

Equation 6 must be solved for gradually smaller values of s until the solution converges. With the lifetime of the primary biradical being shorter than 1 μs, a value of $s = 0.1$ s^{-1} turns out to be satisfactory as the smallest step.[5] For the comparison with the experimental data in the figures, the calculated CIDNP dependencies were normalized to unity at their maximum.

The SNP decay time is calculated as follows. First, the Hamiltonian of the system is modified for the case of the interaction of the electron spin with the microwave field as described earlier:[10]

$$\hat{H} = \hat{H}_0 + \hat{H}_1(t) \quad (7)$$

where $\hat{H}_0$ is described by eq 2 and

$$\hat{H}_1(t) = \beta_e\hbar^{-1}B_1[(g_1\hat{S}_{1x} + g_2\hat{S}_{2x})\cos\omega t + (g_1\hat{S}_{1y} + g_2\hat{S}_{2y})\sin\omega t)] \quad (8)$$

In eq 8, B_1 is the amplitude of the pump field and ω its frequency. The time dependence of the Hamiltonian is eliminated as described previously[10] using the standard transformation to a rotating frame of reference (RFR) by means of the rotation operator $\hat{M}_1$

$$\hat{M} = e^{-i\omega\hat{F}_z t}, \quad \hat{F}_z = \hat{S}_{1z} + \hat{S}_{2z} + \hat{I}_z \quad (9)$$

yielding

$$\hat{H}_{1RFR} = \beta_e\hbar^{-1}B_1(g_1\hat{S}_{1x} + g_2\hat{S}_{2x}) \quad (10)$$

The operators $\hat{\mathbf{R}}$, $\hat{\mathbf{W}}$, $\hat{\mathbf{K}}$ in eq 1 are axially symmetric and stay unchanged under transformation to RFR. As in case of the CIDNP calculation, the SLE (1) is solved using the Laplace transformation of the spin density matrix. The biradical lifetime is calculated from the geminate product yield $P(s)$:[5]

$$\tau = \frac{P(0) - P(s)}{sP(s)} \quad (11)$$

with

$$P(s) = k_r[\rho_{S\alpha S\alpha}(s)|_{r=r_d} + \rho_{S\beta S\beta}(s)|_{r=r_d}] + k_{soc}\sum_i [\rho_{T_i\alpha T_i\alpha}(s)|_{r=r_d} + \rho_{T_i\beta T_i\beta}(s)|_{r=r_d}] \quad (12)$$

Discussion

As was mentioned in the previous sections, two types of biradicals (acyl−alkyl and bis-alkyl) are generated after photoexcitation of the starting ketone **I**. Two important points concerning the difference between the biradicals under study are to be considered more explicitly. First, the structure of one of the radical paramagnetic centers is different; namely, the acyl group is present in the primary biradical only. Second, these biradicals differ in the number of molecular bonds linking the radical centers. The primary acyl−alkyl biradicals have 12 and the secondary bis-alkyl biradicals have 11 methylene groups. As a consequence, bis-alkyl biradicals have a smaller average distance between the radical centers and thus the larger average exchange interaction. Accordingly, B_0^{max} in the shorter C_{11} bis-alkyl biradical is shifted to higher magnetic field with respect to the C_{12} acyl−alkyl biradical. As far as the structural difference of the radical centers is concerned, our previous investigations of biradical reactions during the photolysis of mono- and dihydroxy-substituted cyclic ketones have revealed a strong influence of the carbonyl group on the intersystem crossing.[8b−d] As has been shown, the presence of the acyl radical center provides a spin−orbit coupling which is sufficiently strong to be an efficient channel of ISC and thus reduces the importance of the nuclear spin-dependent channel of singlet−triplet mixing. Hence, the difference in biradical structures of the involved biradicals is expected to affect the formation of spin polarization in the products.

The variation of temperature has an influence on several physical properties which are important for the formation of spin polarization. Examples are (i) the molecular dynamics, (ii) the correlation times relevant for relaxation by different mechanisms, (iii) the statistical distribution function for the interradical distance, and (iv) the decarbonylation rate constant, which determines the ratio of primary and secondary biradicals in the reaction. In comparison, the solvent viscosity variation has an influence only on a subset of the parameters, and the effect of hyperfine interaction is independent of the medium.

At room temperature and below, the normalized ^{13}C CIDNP field dependencies of signals of the quaternary carbon atoms (i.e., signals 3−5 corresponding to ^{13}C positions with equal hfi constants in both intermediates) coincide within the experimental error. Also, the field dependencies of all ^{1}H CIDNP signals fall on the same curve. The coincidence of the ^{1}H and ^{13}C CIDNP field dependencies of the signals, the polarization of which is formed in the primary biradical only (signals 4 and 5 for ^{13}C, and the aldehyde proton signal), and of the signals with contributions of CIDNP from both, primary and secondary, biradicals (signal 3 for for ^{13}C, and the methyl and methylene protons signal) accords with the small probability of the reaction pathway via the bis-alkyl biradical in this temperature range. Our estimation of the rate constant for the decarbonylation reaction at room temperature is k_{co}=3 × 10^5 s^{-1},[8a] and this rate is much smaller than the acyl−alkyl biradical decay rate of about 1.44 × 10^7 s^{-1} as obtained from an exponential fit of the ^{1}H SNP data at room temperature.

In the model, the whole set of the parameters describing the spin and molecular dynamics can be divided into two groups: in the first group are those, which are dependent on the temperature and viscosity, and in the second group are those that do not change with the medium parameters but depend only

on the nucleus under observation. To the first group belong the correlation times τ_u and τ_c describing the relaxation processes, the shape of the distribution function *C(r)*, and the effective diffusion coefficient D' describing the molecular dynamics of the biradical, which changes under temperature and solvent viscosity variation. The rate k_{soc}, the parameters describing the exchange interaction J_0 and α, and the fluctuating magnetic field components for the uncorrrelated relaxation *G*, are considered to be independent of the medium and of the nucleus (proton or carbon). The hyperfine coupling constants for carbon are taken from literature,[12] and for protons we used an effective value of $A = 3.0$ mT.

Our calculations show that for the products of primary biradicals the main factor for the changes in the field dependence of CIDNP and in the SNP decay times is the variation of the effective diffusion coefficient D' with temperature. Therefore D' was used as fitting parameter. The fitting strategy applied in our calculations includes the following steps: (1) for simulating the ^{1}H and ^{13}C CIDNP field dependencies at room temperatures, for a given viscosity, a common set of parameters is optimized except for the hyperfine couplings where the appropriate value for each nucleus is taken; (2) the same parameter set is checked that it reproduces the SNP decay; (3) by variation of only D' and the correlation times the best fit for ^{1}H and ^{13}C CIDNP field dependencies and for the ^{1}H and ^{13}C SNP decays of the primary biradical is evaluated for the whole range of temperature and viscosity.

For the model calculations of the CIDNP field dependence at room temperature, we used as starting values the same set of the main parameters as found in our previous studies.[8b] Good agreement between experiment and calculation was obtained for the ^{1}H and ^{13}C data (Figures 1b and 4a) after a slight adjustment of D'. The best fit was obtained with the effective diffusion coefficient $D' = 3 \times 10^{-5}$ cm^2 s^{-1}, the correlation times $\tau_c = 8 \times 10^{-11}$ s and $\tau_u = 1 \times 10^{-12}$ s, for the solvent chloroform at room temperature ($\eta = 0.58$ cP, $T_0 = 298$ K). The fact that D' is slightly larger than for acyl−ketyl biradical in methanol ($D' = 2 \times 10^{-5}$ cm^2 s^{-1})[8b] might be attributed to the hydrogen bonding of the OH groups with the methanol. All the other parameters are essentially the same as found earlier.[8b]

The time-resolved SNP measurements at room temperature demonstrate the crucial role of the nuclear spin independent channel of ISC in the primary biradical due to the spin−orbit coupling provided by the acyl radical center. The decay rate of all signals observed by ^{1}H and ^{13}C SNP for protonated and deuterated compounds is virtually the same. In principle, the substitution of protons by deuterons leads to a decrease of the efficiency of ISC due to the decrease of hyperfine interaction. As a result, the decay time of the SNP signal is expected to be longer for the deuterated compounds. Likewise the presence of the magnetic isotope ^{13}C in the positions with large hyperfine interaction constants is expected to accelerate the SNP decay. However, such an effect was not observed in our experiments. This result leads us to the conclusion that the hyperfine interaction induced channel of ISC is only of minor importance for the spin evolution of the acyl−alkyl biradical.

Rising the temperature has only a minor influence on the ^{1}H CIDNP field dependence of the products of the primary biradical. In contrast, with increasing temperature a considerable broadening of the ^{1}H CIDNP field dependencies and a shift of their emission maximum toward higher field is observed for the vinyl and aliphatic protons, the polarization of which is formed in both primary and secondary biradicals. A similar observation is made for ^{13}C CIDNP: upon heating the field dependencies for signals 4 and 5 change only slightly, while the emission maximum for signal 3 is strongly shifted toward higher magnetic field. The change of B_0^{max} with temperature for signals, which have contributions from products of both biradicals ("mixed" lines), can mainly be attributed to the increase of the part from the secondary biradical. In addition, we can conclude from our data that temperature variation has a larger effect on the bis-alkyl biradical than on the acyl−alkyl biradical. In the high-temperature range the molecular motion of the polymethylene chain is fast (the reencounter rate, estimated as $k_{re} = 2D'/(r_{max} - r_{min})^2$, is about 10^{10} s^{-1}). Admixture of singlet character induced by hfi is very effective for the T_ sublevel; therefore, the rate-limiting step of the triplet biradical decay is the decay of the T_+ and T_0 sublevels. They are coupled with the S and T_ states by electron paramagnetic relaxation, and with the S state by short-range spin−orbit interaction. The latter is of importance for the acyl−alkyl biradical only. Model calculations show that the shape of the field dependence can, in principle, be affected by the electron paramagnetic relaxation in the biradical and by the molecular dynamics in a very similar way. The increase of the effective diffusion coefficient, which is expected with increasing temperature, leads to broadening of the field dependence and to the shift of its emission maximum toward higher field. The decrease of the correlation times with increasing temperature can cause similar changes. However, the presence of significant spin−orbit coupling, itself having no direct temperature dependence, reduces the importance of electron relaxation and hfi-induced intersystem crossing for the spin evolution of the biradical. Therefore it is expected to reduce strongly the effect of temperature on the CIDNP field dependencies. The introduction of spin−orbit coupling into our calculation with the rate $k_{soc} = 2.2 \times 10^9$ s^{-1} at the nearest interradical distance, as was found in our previous work,[8b] allows us to simulate the observed influence of the temperature on the field dependence of CIDNP in the products of the primary acyl−alkyl biradical. Good quantitative agreement between experiment and calculation is obtained for the field dependence of both proton and carbon polarization of the primary products using an identical set of parameters except for the values of A_{eff} which are 3.0 mT for the aldehyde proton (Figure 1a) and 4.6 mT for the quaternary carbons and 11.4 mT for carbonyl carbon (Figure 4a). This fact demonstrates that our model can indeed describe very well the spin evolution of the primary biradicals over the full high-temperature range.

Upon heating, only a minor change in the ^{1}H SNP decay for the primary products is observed. This fact leads us to the conclusion that in this temperature range the decarbonylation rate still remains small in comparison with the decay rate of the acyl−alkyl biradical, which is mainly determined by SOC. The identical values of the initial SNP amplitude K^0_{SNP} for the contribution from the primary biradical to the aldehyde and to the $=CH_2$ signal reflect the fact that the protons at the alkyl end of the biradical have the same hfi constant and that only one of the spins flips in the S−T_ transition. Comparison of K^0_{SNP} for the signals of the aldehyde and the $=CH_2$ protons shows that, in the secondary biradical, although it gives only a minor contribution to the reaction, a significant nuclear spin polarization is formed. This is not surprising since in the bis-alkyl biradical spin−orbit coupling, usually resulting in the reduction of magnetic and spin effects, does not play any important role. The increase of the ^{1}H SNP decay time with temperature for signals having contributions from both primary and secondary biradicals is also in agreement with the fact that

the SOC does not contribute much to the bis-alkyl biradical decay, and that the lifetime of the bis-alkyl biradical is, therefore, mainly determined by hfi and electron relaxation.

In the temperature range below 280 K, polarization is detected only for products formed from the primary biradical. Upon further cooling, the emission maximum of the ^{1}H CIDNP field dependence changes its position and below 240 K, in particular in the range between 203 and 220 K, ΔB, the width of the field dependence, gets substantially larger with cooling. This change is accompanied by a considerable increase of the SNP decay time. It is reasonably to assume that the temperature induced changes observed in SNP and CIDNP are due to the decrease of the molecular mobility. In our model, this property is taken into account as decrease of the effective diffusion coefficient D' and of the correlation (τ_u and τ_c) times for the primary biradical. The substantial broadening of the field dependence indicates that the reencounter rate becomes small in comparison with the intersystem crossing rate.

To check whether the experimental data in the whole temperature range can be described by an Arrhenius type of temperature dependence, we performed model calculations using the same set of temperature independent parameters (J_0, α, A, g_1, g_2, G, k_r, and k_{soc}) as in the high temperature range, varying only the values of τ_u and D' in the following way:

$$D' = D'_0 \exp\left(-\frac{E}{R}\left(\frac{1}{T}-\frac{1}{T_0}\right)\right) \qquad \tau_u = \tau_{u0} \exp\left(\frac{E}{R}\left(\frac{1}{T}-\frac{1}{T_0}\right)\right) \tag{13}$$

where $\tau_{u0} = \tau_u(298\ \mathrm{K}) = 1 \times 10^{-12}$ s, $T_0 = 298$ K, $D'_0 = D'(298\ \mathrm{K}) = 3 \times 10^{-5}$ cm^2 s^{-1}, $E = 16.7$ kJ/mol. We assume that τ_u and D' have the same activation energy which is determined by the rotation barrier around a C−C bond. For the effective barrier we used the average value of the three energy barriers for rotationally isomeric states of the polymethylene chain,[5] which were used for the *C(r)* calculation. The same energy barrier was obtained from the fitting of ΔB for the ^{1}H CIDNP field dependence in the low-temperature range by variation of D'. For the temperature dependence of τ_c we used the expression $\tau_c = \tau_{c0}(T_0/T)(\eta/\eta_0)$ where $\eta_0 = \eta(298\ \mathrm{K}) = 0.58$ cP and $\tau_{c0} = \tau_c(298\ \mathrm{K}) = 8 \times 10^{-11}$ s. It was shown previously that the proportionality $\tau_c \propto \eta/T$ gives a good description of the CIDNP biradical kinetics at variable temperature.[13]

However, the variation of temperature causes more changes than described so far. The calculation shows that variation of only the above-mentioned parameters (D', τ_c, and τ_u) with temperature makes it impossible to describe all results obtained in the whole temperature range. Only at room temperature and above, when the molecular dynamics of the biradical is fast, good quantitative agreement between the model calculation and the experimental data for carbon and proton spin polarization is achievable. At low temperatures, to avoid systematic deviations between calculations and experimental data, it is necessary to introduce in addition a temperature dependence of k_r and k_{soc}. The reason for this may be the following: the mutual orientation of acyl and alkyl unpaired electron orbitals is important for the recombination,[15] and probably, orientations favorable for reaction become less populated at low temperature. Since in our model the orientation dependence of the reaction rates is not taken into account, we introduce an Arrhenius type dependence for k_r and k_{soc}. In our calculation, we use in the temperature range of 203−298 K the same activation energy ($E = 16.7$ kJ/mol) for both rate constants as we used for D' and τ_u. With this reasonable assumption, the systematic deviation between experimental data and model calculation in the low-temperature range disappears and good agreement between the calculated and experimental data is achieved for both, the ^{1}H field dependencies and the decay times of the SNP signals, in the whole (low and high) temperature range between 203 and 353 K. This is a remarkable achievement allowing to conclude that the single parameter set and the Arrhenius type of its temperature dependence can reliably describe the time and field dependencies of nuclear polarization in this wide temperature range. For the convenience of the readers, we collect in Table 2 the parameter values used for the calculation as presented in the Figures.

TABLE 1: Common Set of the Parameters

g_1 (acyl)	g_2 (alkyl)	G, s^{-2}	J_0, T	α, Å^{-1}
2.0026	2.0008	8×10^{16}	-7×10^5	2.14

TABLE 2: Parameter Values Used for Simulations as Presented in the Figures

T, K	D, cm^2 s^{-1}	τ_u, s	τ_c, s	k_r, s^{-1}	k_{soc}, s^{-1}
203	1.3×10^{-6}	2.3×10^{-10}	8.1×10^{-10}	4.3×10^9	9.5×10^7
222	3.0×10^{-6}	1.0×10^{-11}	4.0×10^{-10}	1.0×10^{10}	2.2×10^8
273	1.6×10^{-5}	1.8×10^{-12}	1.0×10^{-10}	5.4×10^{10}	1.2×10^9
298	3.0×10^{-5}	1.8×10^{-12}	8.0×10^{-11}	1.0×10^{11}	2.2×10^9
353	8.5×10^{-5}	1.0×10^{-13}	3.5×10^{-11}	1.0×10^{11}	2.2×10^9

In the frame of our model the effective diffusion coefficient describing the molecular dynamics of the biradicals drops exponentially with ($1/T$) when the temperature decreases. On one hand, such an Arrhenius-like behavior can be interpreted as a sign that the molecular mobility of the polymethylene chain is predominantly an intramolecular temperature activated process which is not controlled by the solvent viscosity. In combination with the result that no quantitative agreement between experimental data and the model calculation is obtainable without adjusting k_r and k_{soc}, it indicates that anisotropy of the reactivity is very important at low temperatures. On the other hand, for such small values of D', the de Kanter/Kaptein diffusional model[5] for the description of the molecular mobility may not be applicable anymore. Also, it is possible that in this temperature range the anisotropic parts of hyperfine and of exchange interaction as well as of dipole−dipole interaction between the unpaired electron spins, which are not included into our Hamiltonian assuming that they are averaged by fast molecular tumbling, become to be important.

In this paper we restrict ourselves to model calculations of the spin polarization in the primary biradical. However, our model can be extended to include two sequential biradical stages. The computational efforts stay feasible if the nonsecular parts of the hyperfine interaction are taken into account for only one magnetic nucleus. Preliminary results show that in this case the spin dynamics in the secondary biradical is considerably underestimated, and therefore, the resulting polarization for the products of the secondary biradical has too low an amplitude. With a reasonable set of the parameters it was not possible to get qualitative agreement with the experimental data for the polarization formed in the secondary stage. The necessary extension of the model to a minimum number of two nuclei with spin $I = {}^1/_2$ leads to a considerable increase of the dimension of the matrixes in the SLE, from 64 to 256. Such calculations are in progress in our laboratories.

As an alternative we checked the often applied two state model with a constant value of the exchange interaction $\langle J \rangle$, but it completely failed to reproduce the experimental data obtained in a large temperature range. Therefore we can conclude that it is worth the effort to use the more sophisticated model of flexible biradicals which describes the spin and

molecular dynamics as coupled together via the distance dependence of the exchange interaction.

Conclusion

Our experimental results and model calculations demonstrate that low magnetic field CIDNP and SNP are very sensitive to the influence of the different dynamic processes. The changes of CIDNP and SNP effects in the primary and the secondary reaction products at high temperature directly reflect the changes in the reaction branching ratio. Time resolved SNP allows to estimate the lifetime of different biradical intermediates. The invariance of the SNP decay time of the acyl−alkyl biradical with respect to isotope substitution indicates that ISC is mainly determined by nuclear spin independent processes. For the secondary biradical, our results strongly support the conclusion that the nonspin-selective channel of ISC is comparatively weak in the bis-alkyl biradicals. It turned out that our work allows to sensitively test the model used for the description of the molecular dynamics of the polymethylene chain in the wide temperature range. At room temperature and above, when the molecular dynamics of the biradical is fast, quantitative agreement between the model calculation and the experimental data is achievable. At low temperatures, when the molecular dynamics becomes slow, the assumption of reduced reactivity allows to extend the quantitative description to the whole temperature range and to reproduce the main features of the biradical evolution. An extension of the model for taking into account the magnetic interaction with two nuclei and in two consecutive biradicals is in progress

Acknowledgment. We thank Herbert Zimmermann, Max Planck Institute, Heidelberg (Germany), for the synthesis of the 2,2,12,12-tetramethylcyclododecanone and its deuterated isotopomer. Financial support from the Deutsche Forschungsgemeinschaft (Sfb 337), RFBR (Project 96-03-32930), INTAS (project 96-1269) is gratefully acknowledged. One of us (A.Y.) expresses thanks to the Alexander von Humboldt Foundation for her research fellowship at the Free University of Berlin.

References and Notes

(1) (a) Jonston, L. J.; Scaiano, J. C. *Chem. Rev.* **1989**, *89*, 521 and references therein. (b) Doubleday, C., Jr.; Turro, N. J.; Wang, J.-F. *Acc. Chem. Res.* **1989**, *22*, 199 and references therein. (c) Steiner, U. E.; Wolff, H.-J. In *Photochemistry and Photophysics*, Rabek, J. F., Ed., CRC Press: Boca Raton, 1991; p 68.

(2) (a) Closs, G. L.; Doubleday, C. E. *J. Am. Chem. Soc.* **1973**, *89*, 521. (b) Closs, G. L. *Adv. Magn. Reson.* **1974**, *7*, 157.

(3) (a) Closs, G. L.; Forbes, M. D. E.; Piotrowiak, P. *J. Am. Chem. Soc*. **1992**, *114*, 3285. Closs, G. L.; Forbes, M. D. E. *J. Am. Chem. Soc.* **1987**, *109*, 6185. (c) Closs, G. L.; Forbes, M. D. E. *J. Phys. Chem*. **1991**, *95*, 1924.

(4) Han, N.; Hwang, K. C.; Lei, X.; Turro, N. J. *J. Photochem. Photobiol. A* **1991,** *61*, 33.

(5) De Kanter, F. J. J.; den Hollander, J. A.; Huizer, A. H.; Kaptein, R. *Mol. Phys.* **1977**, *34*, 857.

(6) (a) Maeda, K.; Terazima, M.; Azumi, T.; Tanimoto, Y. *J. Phys. Chem.* **1991**, *95*, 197. (b) Maeda, K.; Meng, Q.-X.; Aizawa, T.; Terazima, M.; Azumi, T.; Tanimoto, Y. *J. Phys. Chem.* **1992**, *96*, 4884.

(7) (a) Zimmt, M. B.; Doubleday, C., Jr.; Turro, N. J. *J. Am. Chem. Soc*. **1985**, *107*, 6724. (b) Zimmt, M. B.; Doubleday, C., Jr.; Turro, N. J. *J. Am. Chem. Soc.* **1986**, *108*, 3618. (c) Zimmt, M. B.; Doubleday, C., Jr.; Turro, N. J. *Chem. Phys. Lett.* **1987**, *134*, 549. (d) Wang, J.-F.; Doubleday, C., Jr.; Turro, N. J. *J. Am. Chem. Soc.* **1989**, *111*, 3962. (e) Wang, J.-F.; Rao, V. P.; Doubleday, C., Jr.; Turro, N. J. *J. Phys. Chem.* **1990**, *94*, 1144.

(8) (a) Morozova, O. B.; Yurkovskaya, A. V.; Tsentalovich, Yu. P.; Vieth, H.-M. *J. Phys. Chem. A* **1997**, *101*, 399. (b) Tsentalovich, Yu. P.; Morozova, O. B.; Avdievich, N. I.; Ananchenko, G. S.; Yurkovskaya, A. V.; Ball, J. D.; Forbes, M. D. E. *J. Phys. Chem*. A **1997**, *101*, 8808. (c) Morozova, O. B.; Yurkovskaya, A. V.; Tsentalovich, Yu. P.; Sagdeev, R. Z.; Wu, T.; Forbes, M. D. E. *J. Phys. Chem*. A **1997**, *101*, 8803.

(9) Bagryanskaya, E. G.; Sagdeev, R. Z. *Prog. React. Kinet.* **1993**, *18*, 63.

(10) Koptyug, I. V.; Lukzen, N. N.; Bagryanskaya, E. G.; Doktorov, A. B.; Sagdeev, R. Z. *Chem. Phys.* **1992**, *162*, 165.

(11) (a) Dvinskikh, S. V.; Yurkovskaya, A. V.; Vieth, H.-M. *J. Phys. Chem*. **1996**, *100*, 8125. (b) Dvinskikh, S., Egorov, A., Vieth, H.-M. *Appl. Magn. Reson*, **1997**, *12*, 465.

(12) *Magnetic Properties of Free Radicals*; Landolt-Börnstein, New Series, Group II; Fischer, H., Hellwege, K.-H., Eds.; Springer-Verlag: Berlin, 1977; Vol. 9b.

(13) Yurkovskaya, A. V.; Tsentalovich, Yu. P.; Lukzen, N. N.; Sagdeev, R. Z. *Res. Chem. Intermed.* **1992**, *17*, 145.

(14) Lal, M.; Spenser, D. *Mol. Phys.* **1971,** *22*, 649.

(15) De Kanter, F. J. J.; Kaptein, R. *J. Am. Chem. Soc.* **1982**, *104*, 4759.